HHS Public Access

Author manuscript

J Orthop Res. Author manuscript; available in PMC 2019 August 06.

Published in final edited form as:

J Orthop Res. 2013 August ; 31(8): 1276–1282. doi:10.1002/jor.22355.

Needle Puncture Injury Causes Acute and Long-Term Mechanical Deficiency in a Mouse Model of Intervertebral Disc Degeneration

John T. Martin[1,2], **Deborah J. Gorth**[1], **Elizabeth E. Beattie**[1,2], **Brian D. Harfe**[3], **Lachlan J. Smith**[1], **Dawn M. Elliott**[4]

[1]Department of Orthopaedic Surgery, University of Pennsylvania, Philadelphia, Pennsylvania, 19104

[2]Department of Mechanical Engineering and Applied Mechanics, University of Pennsylvania, Philadelphia, Pennsylvania, 19104

[3]Department of Molecular Genetics and Microbiology, The Genetics Institute, University of Florida, Gainesville, Florida, 32610

[4]Department of Biomedical Engineering, University of Delaware, Newark, Delaware, 19716

Abstract

Low back pain is a significant socioeconomic burden and intervertebral disc degeneration has been implicated as a cause. A reliable animal model of disc degeneration is necessary to evaluate therapeutics, and functional metrics are essential to quantify their benefit. To this end, needle puncture injuries were created in the caudal intervertebral discs of mice to induce disc degeneration. Compression, torsion, and creep mechanics were assessed both immediately and after eight weeks to distinguish between the effects of injury and the subsequent reparative or degenerative response. Two needle sizes (29 and 26 gauge) were used to determine injury size-dependence. Compressive stiffness (62%), torsional stiffness (60%), and early damping stiffness (84%) decreased immediately after injury with the large needle (26G). These mechanical properties did not change over time despite structural and compositional changes. At 8 weeks following large needle injury, disc height decreased (37%), nucleus pulposus (NP) glycosaminoglycan content decreased (41%), and NP collagen content increased (45%). The small needle size had no significant effect on mechanics and did not initiate degenerative changes in structure and composition. Thus, the injection of therapeutics into the NP with a minimal needle size may limit damage due to the needle insertion. These findings, along with the wide commercial availability of mouse-specific biological probes, indicate that the mouse caudal disc model can be a powerful tool for investigating disc degeneration and therapy.

Keywords

intervertebral disc; degeneration; injury; mechanics; mouse

Correspondence to: Dawn M. Elliott (T: 302-831-1295; delliott@udel.edu).

The intervertebral disc has been implicated as a cause of low back pain, which accounts for ~100 billion dollars in medical costs, lost wages, and decreased productivity in the United States.[1] While current surgical and non-surgical interventions may relieve discogenic pain, they do not restore disc function. An in vivo disc degeneration model can provide a platform for evaluating therapies aimed at reducing pain *and* restoring function. Because the primary function of the disc is mechanical, consideration of disc mechanics is critical in such models.

Intervertebral disc injury in animal models consistently produces an acute response that progresses to resemble key features of human disc degeneration.[2,3] Injury models provide repeatable results and have controlled specificity in comparison to global gene knockouts and spontaneous development models. Thus, injury studies have been conducted in many species including sheep, pig, rabbit, and rat.[4–9] Methods for inducing degeneration through injury include scalpel incision, defect creation (box, cruciate), and needle puncture; of these methods, needle puncture is used frequently as it depressurizes the nucleus pulposus (NP), a primary factor for creating instability, while also minimizing annulus fibrosus (AF) damage.[6,7,9] Recently, the mouse caudal disc was shown to degenerate as a result of needle puncture, displaying changes in morphology, cellularity, and composition consistent with those in humans.[10] Puncture-initiated degeneration of the rodent caudal disc requires only minor surgery; thus, it is an excellent alternative to the invasive and technically challenging peritoneal or dorsolateral approach of lumbar surgery.[11] The mouse caudal disc is also comparable mechanically to the human lumbar disc when accounting for geometry, despite different physiological loading environments.[12,13] These factors, along with the wide commercial availability of mouse-specific biological assays, indicate that the mouse caudal disc model can be a powerful tool for investigating degeneration and therapy.

Restoring mechanical function is the end-goal of potential therapies and thus is the primary metric for studying their efficacy. Mechanical changes immediately following puncture[9,14,15] and over time due to biological effects such as inflammation[5,6] were assessed in separate studies; however, no study has linked the immediate mechanical changes with progressive mechanical deterioration or recovery. A needle diameter to disc height ratio of 40% is required to cause changes in the mechanics of *lumbar* discs,[15] while much larger defects are required to alter rat *caudal* disc mechanics.[9,14] By evaluating acute and long-term disc mechanics, changes caused by the initial puncture can be distinguished from those caused by physiological processes, and, by evaluating needle sizes, an appropriate injury for a degeneration model can be selected.

Mechanical data for the degenerate mouse disc is currently limited to bending and creep[16,17]; however, compression and torsion are also primary mechanical modes. They are governed by different structural mechanisms, compression through the interactions between the NP and AF, and torsion primarily through loading of the AF fiber network. Quantification of the compressive and torsional mechanical behavior of healthy and degenerate discs will aid in understanding alterations in mechanics of the individual disc tissues.

We quantified the acute and long-term effects of needle puncture injury on mouse caudal disc function. Injuries were induced with two needle sizes and were evaluated for changes in disc structure, mechanics, and composition both immediately and after eight weeks. We hypothesized that the puncture would decrease compressive and torsional mechanical properties and that these changes would be amplified by subsequent structural and compositional deterioration.

METHODS

Surgical Procedure

With institutional IACUC approval, 26 C57BL/6 retired breeder mice (7.5–9 months, 32.7 ± 5.1 g) were obtained from Jackson Laboratories (Bar Harbor, ME) and allocated to two time points: 0 weeks (n = 12) and 8 weeks (n = 14). Mice were anesthetized in an aseptic setting, and the surgery was fluoroscopically guided. The C6/C7 and C8/C9 discs were exposed with a 2.5 mm dorsal longitudinal scalpel incision, and puncture injuries were created at a randomly assigned level with either a 29G (65% of disc height) or 26G (90% of disc height) needle, while the other exposed disc served as a sham control. Needles were inserted at the dorsal annulus through the NP center and partially through the ventral annulus (controlled depth of 1.75 mm or 90% of the dorsoventral width) for 30 s and removed. The injured level was marked with India ink, and both incisions were closed with suture. Mice were returned to normal cage activity and euthanized after 8 weeks. Zero-week mice were euthanized, and their discs were punctured in vitro following the same procedure.

Microcomputed Tomography

mCT (vivaCT 40, SCANCO Medical AG, Bruttisellen, Switzerland) was used to measure disc area and mean disc height of 0-week control and 8-week control and punctured groups (n = 7/group). The C6 through C9 section of the caudal spine was removed and imaged en bloc at an isotropic 21 μm resolution. Volumetric image data were converted to stacks of cross-sectional vertebral body slices, and disc area and mean disc height were measured from a 3D reconstruction of slices that spanned the disc space[11] (Fig. S1, a–c). Polar moment of inertia, J_z, about the spinal longitudinal axis was measured from a cross-sectional slice directly distal to the disc space for use in normalizing torsional mechanical properties (Fig. S1, d–f).

Mechanical Testing

Mechanical function was assessed with an electromechanical testing system (Instron 5542, Instron, Norwood, MA) fit with a custom torsion device consisting of a stepper motor (AM1524; MicroMo Electronics, Inc., Clearwater, FL) and a 5 in.-oz (35 mN m) torsional load cell (TFF400; Futek, Irvine, CA) (Fig. 1a). A custom LabVIEW (LabVIEW 8.5; National Instruments, Austin, TX) program was used to control the angular displacement of the stepper motor and read the torsional reaction force. While the testing system and stepper motor directly controlled the compressive and rotational displacements, two digital cameras (A602f; Basler, Exton, PA) were used to optically track the extension and rotation of each vertebral body (Fig. 1b). Axial position (mm) was defined as the difference in the z-position of points in camera 1, while rotational position (radians) was measured by recording the x-

position of a point in camera 1 and the *y*-position of the same point in camera 2 and defined as $\tan^{-1}(y/x)$ (Fig. 1c). A significant portion of machine-reported displacement was a contribution of unavoidable motion at spots along the load string (e.g., slipping at the grips or motions between bolted connections to the load cell), and, because the rodent disc is small, these motions had a relatively large impact. Thus, displacement error was eliminated through optical tracking with the dual camera system and a custom texture tracking program written in Matlab. Preliminary evaluations of this technique demonstrated that axial displacements and rotations were successfully captured as 85.4 ± 12.4% and 75.4 ± 38.4% of their machine-reported counterparts, respectively (Fig. 2). These optical measures were used in post-test mechanical parameter calculations.

Discs from 0-week control to 8-week control and punctured groups (n = 5/group) were exposed to compressive, creep, and torsional loads. Caudal spines were prepared as bone-disc-bone segments by cutting through adjacent unused discs (leaving the entire vertebral body surface area to grip for mechanical testing) and gently clearing extraneous tendon and muscle with a scalpel. The protocol consisted of 20 cycles of compression/tension from −1.5 to +0.5N at 0.5 Hz[18] (causing compression/extension of the disc from ~70 to 130% of the initial height), a 1 h creep load of −1.5N,[18] and 10 cycles of torsion of ±8° at 0.05 Hz.[12] All testing was conducted in phosphate-buffered saline bath at room temperature.

Compression/tension data were analyzed for compressive stiffness and range of motion (ROM), and neutral zone (NZ) stiffness and ROM by fitting data to a sigmoid function[19] (an S-shaped curve with well-behaved 1st and 2nd derivatives that represents displacement as a function of applied load) (Fig. 3). Compressive and NZ stiffness were normalized by multiplying by the disc height and dividing by the disc area,[18] and ROM measurements were normalized by dividing by the disc height.[18] Torsion data were analyzed for torsional stiffness, torque range, torsional NZ stiffness and torsional NZ ROM using the same curve fitting procedure (Fig. 3). Torsional stiffness, torsional NZ stiffness, and torque range were normalized by multiplying by the disc height and dividing by J_z.[12]

Creep behavior was fit to a 5-parameter viscoelastic constitutive model[20]

$$d(t) = \frac{L}{S_1}(\mathbf{1} - e^{-t/\tau_1}) + \frac{L}{S_2}(\mathbf{1} - e^{-t/\tau_2}) + \frac{L}{S_3} \quad (1)$$

describing the displacement (d) at time (t) for constant load (L). The material response consists of an elastic stiffness (S_3) and two exponential decays with one time constant (τ_1, τ_2) and damping stiffness (S_1, S_2) each. This model provided a simple but reasonable method to compare the time-dependent response across groups. Creep displacement was measured from raw optical displacement. Damping stiffnesses were normalized by multiplying by disc height and dividing by disc area, and creep displacement was normalized by dividing by disc height.[18]

NP Glycosaminoglycan (GAG) and Collagen Content

Following mechanical testing, discs from 0-week control and 8-week control and punctured groups (n = 5/group) were isolated for NP GAG and collagen content analysis. First, a scalpel was used to cut through a vertebral body adjacent to the disc above the endplate. The remaining vertebral body-disc segment was embedded in optimum cutting temperature compound on a cryostat microtome, and consecutive sections through the partial vertebral body exposed the underlying disc. A 100 μm section of disc was then isolated, and the NP removed with 0.75 mm biopsy punch (the approximate NP diameter). This technique facilitated precise control of the volume of tissue obtained. Isolated NPs were subsequently digested in papain at 60°C. GAG content was measured using the dimethylmethylene blue (DMMB) technique,[21] and collagen content (following acid hydrolysis) using the p-diamino-benzaldehyde/chloramine-T technique for hydroxyproline[22] assuming a ratio of hydroxyproline to collagen of 1:10.[23] Results are reported as normalized to NP wet weight.

Histology

Discs from 8-week control and punctured groups (n = 2/group) were fixed in formalin, decalcified, and embedded in paraffin. Sagittal, 8 μm sections were stained with alcian blue/picrosirius red for GAG/collagen and imaged under bright field and cross-polarized light.

Statistics

Differences in disc height and GAG and collagen contents were analyzed by one-way ANOVA comparing the 0-week control to the 8-week control and punctured groups. Differences in mechanical properties were analyzed by two-way ANOVA comparing 0-week control and punctured groups to the 8-week control and punctured groups with needle size and time as the main effects. Tukey's post hoc test was used for pairwise comparisons with significance defined as $p \leq 0.05$ and a trend as $0.05 < p \leq 0.10$. Results are reported as mean ± standard deviation.

RESULTS

Mice survived the surgical procedure and recovered with no change in body weight over 8 weeks. Disc height 8 weeks after 26G puncture was less than the 0-week control group (37%, p 0.05), the 8-week control group (29%, $p \leq 0.05$) and the 29G group (28%, $p \leq 0.05$), and there was no significant effect of the sham surgery or 29G needle puncture (Fig. 4a). NP GAG content followed a similar trend as at 8 weeks the 26G group was 41% less than the 0-week control group ($p \leq 0.05$), with no change in 8-week control or 29G groups (Fig. 4b). NP collagen content for the 26G group was not significantly different from 0-week control but was 45% greater than both the 8-week control and 29G groups ($p \leq 0.10$) (Fig. 4c). Histologically, no qualitative differences were noted between control and 29G puncture groups at 8 weeks, while the 26G group had a collapsed disc space, disorganized lamellae, and collagenous NP (Fig. 5).

The baseline mechanical response in both compression and torsion consisted of an elongated low stiffness NZ that transitioned with increasing strain to a high stiffness linear region (Fig. 3). Changes in normalized compressive stiffness, normalized torsional stiffness, and

normalized torque range were a function of puncture size only ($p \leq 0.05$) and not time (Fig. 6). Compressive stiffness of the 26G group was less than the control groups at 0 (62%, $p \leq 0.05$) and 8 weeks (62%, $p \leq 0.05$), but there were no differences across timepoints (Fig. 6a). There were no significant changes in compressive ROM for any treatment (Fig. 6b). Torsional stiffness for the 26G group was significantly less than the control group at 0 (60%, $p \leq 0.05$) and 8 weeks (71%, $p \leq 0.05$), but again there were no differences across timepoints (Fig. 6c). Torque range of the 26G puncture group was less than the control group at 8 weeks (51%, $p \leq 0.05$) (Fig. 6d). The sham surgery and the 29G needle puncture had no effect, and there were no differences in either compressive or torsional NZ mechanics for any of the groups.

The response to creep loading was characterized by an initial high strain rate over the first 60 s and slower strain rate thereafter, equilibrating by ~40 min. Changes in creep properties (normalized S_1, τ_1, τ_2) were a function of puncture size only ($p \leq 0.05$) and not time (Fig. 7). Puncture with 26G needle caused a faster, magnified creep response (Fig. 7a). The early damping stiffness, S_1, of the 26G puncture group was significantly less than the control group at 0 (84%, $p \leq 0.05$) and 8 weeks (84%, $p \leq 0.05$) (Fig. 7d), and there were similar trends for τ_1 and τ_2 (Fig. 7b,c). There were no differences in the late damping stiffness, S_2, the elastic stiffness, S_3, or creep displacement (Fig. 7e).

DISCUSSION

Compression, torsion, and creep mechanics of the mouse caudal disc were assessed both immediately and 8 weeks following needle injury. In each loading modality, stiffness was decreased after puncture with the large needle and remained at those levels at 8 weeks. Conversely, the classical signs of degeneration progressed over 8 weeks: disc height and NP GAG content decreased, while NP collagen content increased, and histological signs of degeneration were present. Thus, needle puncture had an acute effect on mechanics that neither improved nor deteriorated over time despite other compositional changes. In addition, the mouse disc was insensitive to puncture with the smaller needle size. Thus, the injection of therapeutics into the NP with a minimal needle size may limit damage due to the needle insertion.

With disc degeneration the NP undergoes structural and compositional alterations, shifting to a fibrocartilaginous phenotype. We observed this fibrocartilaginous shift—needle puncture triggered compaction of the disc space with subsequent increase in collagen content and reduction in GAG content. This is consistent with findings by Yang et al.,[10] where, following needle injury, the mouse caudal NP transitioned from gelatinous to fibrocartilaginous, shifting from collagen II dominant to collagen I dominant. Results from both studies are consistent with the well-defined alterations in internal composition in human degenerative disc disease.[24] Thus, the mouse disc post-injury might exhibit a distorted internal strain field similar to that of the human degenerate disc.[25] However, bulk segment mechanics declined immediately following puncture, but not over time. The NP transition to fibrocartilage observed here and in human degeneration may represent an adaptation to the loss of AF structural integrity, a physiological response to preserve

segment mechanics or mitigate their decline. Future work should evaluate changes in tissue level mechanics following disc injury.

The immediate effect of needle puncture depends upon the spinal region, as caudal and lumbar discs respond differently to a given defect size. A needle with diameter equivalent to 40% disc height is required to alter the mechanical response of *lumbar* discs in compression.[15] In the *caudal* disc, compressive and torsional mechanics following a 90% disc height disruption (26G) were diminished acutely, while a 65% disc height disruption (29G) had no significant effect. In the rat *caudal* disc, Michalek et al. demonstrated that a 21G needle (80% disc height, assuming a disc height of 1 mm[26]) decreased compressive and torsional properties, while 25G and 30G (50% and 30% disc height) needles affected compression only.[14] Similarly, Hsieh et al.[9] showed that in the rat *caudal* disc an 18G needle (100% disc height) affected compressive properties while 22G and 26G needles (70% and 45% disc height) had no effect. Our results are consistent with these findings, confirming that in the *caudal* disc the defect size threshold is in the range of 80% of disc height. This may be due to lower NP pressure and lower residual AF tension in tail discs compared to lumbar discs, as lumbar levels experience considerable loads due to muscle forces for stance and ambulation.[27]

The immediate changes in torsion mechanics following needle puncture are considered to be needle size-dependent.[14] Torsion is primarily governed by AF fiber tension, which decreases with increasing needle size. The changes in torsion mechanics we measured for the mouse caudal disc are consistent with those of the rat caudal disc.[14] However, no consensus exists regarding the acute changes in compression mechanics following needle puncture, which have been suggested to be both needle size-dependent[15] and size-independent.[14] The underlying theory behind size-independence in compression is that compression mechanics are primarily governed by NP pressure, which may be reduced by puncture regardless of needle size. We could not confirm size-independence in compression (Fig. 6a), which may be due to animal size effects or differences in puncture techniques and mechanical testing protocols. However, changes in compression mechanics may also depend on needle size since, in compression, both NP pressure and AF tension play a fundamental role.

Needle puncture affected the response of the caudal disc to creep loading, although at 8 weeks, the change did not match that of the degenerate human lumbar disc. Puncture with the 26G needle caused a magnified, faster creep response relative to control discs, predominantly seen in the early damping stiffness, S_1. This is similar to the behavior of the rat caudal disc.[9] The stiffness, S_1, dominated the response only over the short term τ_1 (9.3 ± 4.5 s), supporting the idea that puncture results in a pressure vent[28] in which fluid can immediately leave at the onset of load. However, in the human lumbar disc, degeneration causes a magnified and slower response.[29] The late time constant, τ_2, increased with human disc degeneration,[29] which was not the case following needle puncture in the mouse caudal disc.

All animal models have limitations. In this model, while the mechanical effects were immediate and do not represent the slow progressive nature of the human disease, other characteristics of degeneration were controlled and consistent. Also, unlike the human disc,

the mouse disc retains notochordal cells throughout its lifespan,[30] and caudal discs experience different physiological mechanical loading than lumbar discs. Finally, our experiment was not able to reveal a difference in mechanical function following small needle puncture because, for the small effect caused by the 29G needle, the study was underpowered. However, our goal was to initiate a degenerative state and measure the resultant change in mechanics, and the 29G group did not meet any of the criteria for a degenerative state (loss of disc height, loss of NP GAG, and change in histological appearance). Thus, our primary finding that disc height, NP GAG and collagen contents, and mechanical function did not recover 8 weeks after large needle puncture is valid, supporting the mouse caudal injury model for certain studies.

In conclusion, the effects of needle injury in the mouse caudal disc caused an immediate change in mechanics that were not altered over time despite progressive compositional changes. Sufficient mechanical perturbation is required for degenerative changes to occur.[9] Consistent with this theory, changes in mechanics from a large needle injury were associated with downstream alterations in disc height, NP composition, and histological characteristics of degeneration.

Supplementary Material

Refer to Web version on PubMed Central for supplementary material.

ACKNOWLEDGMENTS

Funding was provided by grants from NIH (AR050052, AR055568–02S1, AG029353) and the US Department of Veterans Affairs (I01RX000211). The authors thank Dr. Robert Mauck, Dr. Joseph Sarver, Joseph Chiaro, Katherine Gerasimowicz, and Jessica Balderston for their support. We have no other financial disclosures.

Grant sponsor: NIH; Grant numbers: AR050052, AR055568–02S1, AG029353; Grant sponsor: US Department of Veterans Affairs; Grant number: I01RX000211.

REFERENCES

1. Katz JN. 2006 Lumbar disc disorders and low-back pain: socioeconomic factors and consequences. J Bone Joint Surg 88-A:21–24.
2. Iatridis JC, Michalek AJ, Purmessur D, et al. 2009 Localized intervertebral disc injury leads to organ level changes in structure, cellularity, and biosynthesis. Cell Mol Bioeng 2:437–447. [PubMed: 21179399]
3. Lotz JC. 2004 Animal models of intervertebral disc degeneration: lessons learned. Spine (PhilaPa 1976) 29:2742–2750.
4. Osti OL, Vernon-Roberts B, Fraser RD. 1990 1990 Volvo Award in experimental studies. Anulus tears and intervertebral disc degeneration. An experimental study using an animal model. Spine (PhilaPa 1976) 15:762–767.
5. Kaigle AM, Holm SH, Hansson TH. 1997 1997 Volvo Award winner in biomechanical studies. Kinematic behavior of the porcine lumbar spine: a chronic lesion model. Spine (PhilaPa 1976) 22:2796–2806.
6. Miyamoto K, Masuda K, Kim JG, et al. 2006 Intradiscal injections of osteogenic protein-1 restore the viscoelastic properties of degenerated intervertebral discs. Spine J 6: 692–703. [PubMed: 17088200]

7. Masuda K, Aota Y, Muehleman C, et al. 2005 A novel rabbit model of mild, reproducible disc degeneration by an anulus needle puncture: correlation between the degree of disc injury and radiological and histological appearances of disc degeneration. Spine (PhilaPa 1976) 30:5–14.
8. Rousseau MA, Ulrich JA, Bass EC, et al. 2007 Stab incision for inducing intervertebral disc degeneration in the rat. Spine (PhilaPa 1976) 32:17–24.
9. Hsieh AH, Hwang D, Ryan DA, et al. 2009 Degenerative anular changes induced by puncture are associated with insufficiency of disc biomechanical function. Spine (PhilaPa 1976) 34:998–1005.
10. Yang F, Leung VY, Luk KD, et al. 2009 Injury-induced sequential transformation of notochordal nucleus pulposus to chondrogenic and fibrocartilaginous phenotype in the mouse. J Pathol 218:113–121. [PubMed: 19288580]
11. Boxberger JI, Auerbach JD, Sen S, et al. 2008 An in vivo model of reduced nucleus pulposus glycosaminoglycan content in the rat lumbar intervertebral disc. Spine (PhilaPa 1976) 33:146–154.
12. Showalter BL, Beckstein JC, Martin JT, et al. Comparison of animal discs used in disc research to human lumbar disc: torsion mechanics and collagen content. Spine (PhilaPa 1976) 37:E900–E9007.
13. Elliott DM, Sarver JJ. 2004 Young investigator award winner: validation of the mouse and rat disc as mechanical models of the human lumbar disc. Spine (PhilaPa 1976) 29:713–722.
14. Michalek AJ, Funabashi KL, Iatridis JC. 2010 Needle puncture injury of the rat intervertebral disc affects torsional and compressive biomechanics differently. Eur Spine J 19:2110–2116. [PubMed: 20544231]
15. Elliott DM, Yerramalli CS, Beckstein JC, et al. 2008 The effect of relative needle diameter in puncture and sham injection animal models of degeneration. Spine (PhilaPa 1976) 33:588–596.
16. Court C, Colliou OK, Chin JR, et al. 2001 The effect of static in vivo bending on the murine intervertebral disc. Spine J 1:239–245. [PubMed: 14588327]
17. Palmer EI, Lotz JC. 2004 The compressive creep properties of normal and degenerated murine intervertebral discs. J Orthop Res 22:164–169. [PubMed: 14656676]
18. Beckstein JC, Sen S, Schaer TP, et al. 2008 Comparison of animal discs used in disc research to human lumbar disc: axial compression mechanics and glycosaminoglycan content. Spine (PhilaPa 1976) 33:E166–E173.
19. Smit TH, van Tunen MS, van der Veen AJ, et al. Quantifying intervertebral disc mechanics: a new definition of the neutral zone. BMC Musculoskelet Disord 12:38. [PubMed: 21299900]
20. O'Connell GD, Jacobs NT, Sen S, et al. Axial creep loading and unloaded recovery of the human intervertebral disc and the effect of degeneration. J Mech Behav Biomed Mater 4:933–942. [PubMed: 21783103]
21. Farndale RW, Sayers CA, Barrett AJ. 1982 A direct spectrophotometric microassay for sulfated glycosaminoglycans in cartilage cultures. Connect Tissue Res 9:247–248. [PubMed: 6215207]
22. Stegemann H, Stalder K. 1967 Determination of hydroxyproline. Clin Chim Acta 18:267–273. [PubMed: 4864804]
23. Nimni ME. 1983 Collagen: structure, function, and metabolism in normal and fibrotic tissues. Semin Arthritis Rheum 13:1–86. [PubMed: 6138859]
24. Urban JP, Roberts S. 2003 Degeneration of the intervertebral disc. Arthritis Res Ther 5:120–130. [PubMed: 12723977]
25. O'Connell GD, Vresilovic EJ, Elliott DM. Human intervertebral disc internal strain in compression: the effect of disc region, loading position, and degeneration. J Orthop Res 29:547–555. [PubMed: 21337394]
26. O'Connell GD, Vresilovic EJ, Elliott DM. 2007 Comparison of animals used in disc research to human lumbar disc geometry. Spine (PhilaPa 1976) 32:328–333.
27. Smit TH. 2002 The use of a quadruped as an in vivo model for the study of the spine—biomechanical considerations. Eur Spine J 11:137–144. [PubMed: 11956920]
28. Michalek AJ, Iatridis JC. Penetrating annulus fibrosus injuries affect dynamic compressive behaviors of the intervertebral disc via altered fluid flow: an analytical interpretation. J Biomech Eng 133:084502. [PubMed: 21950904]

29. O'Connell GD, Jacobs NT, Sen S, et al. 2011 Axial creep loading and unloaded recovery of the human intervertebral disc and the effect of degeneration. J Biomech 4:933–942.

30. Smith LJ, Nerurkar NL, Choi KS, et al. Degeneration and regeneration of the intervertebral disc: lessons from development. Dis Model Mech 4:31–41. [PubMed: 21123625]

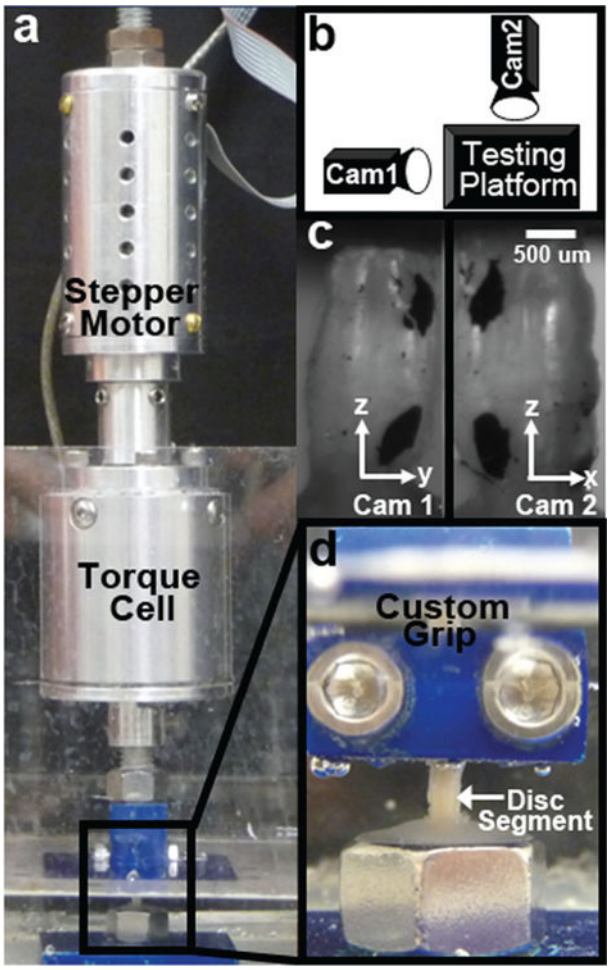

Figure 1.

(a) A custom torsion device consisting of a stepper motor and torque cell was installed on a uniaxial mechanical test system. (b) Two digital cameras positioned 90° apart were used to record the 3D position of the vertebral bodies. (c) Markings on the bodies were tracked with custom software. (d) Samples were fixed to the upper grip, lowered into a pot filled with dental cement and, when cured, the test was started.

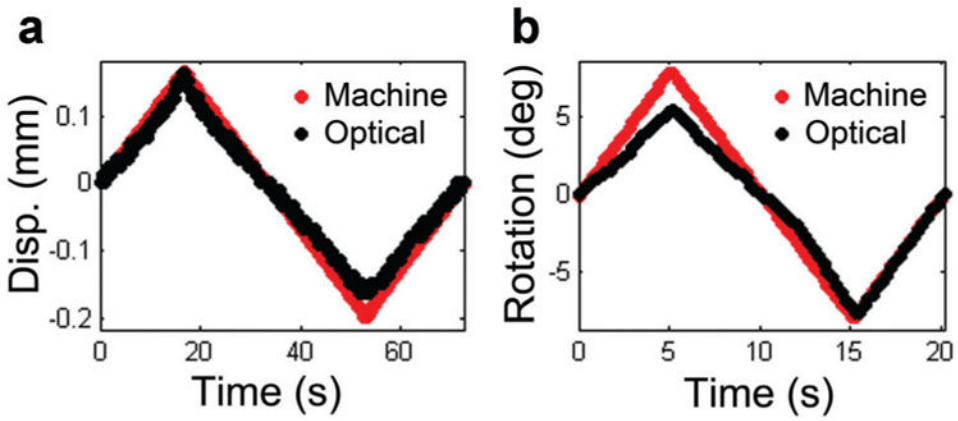

Figure 2.

Representative plots of machine-reported and optically tracked (a) displacement and (b) rotation over a loading cycle.

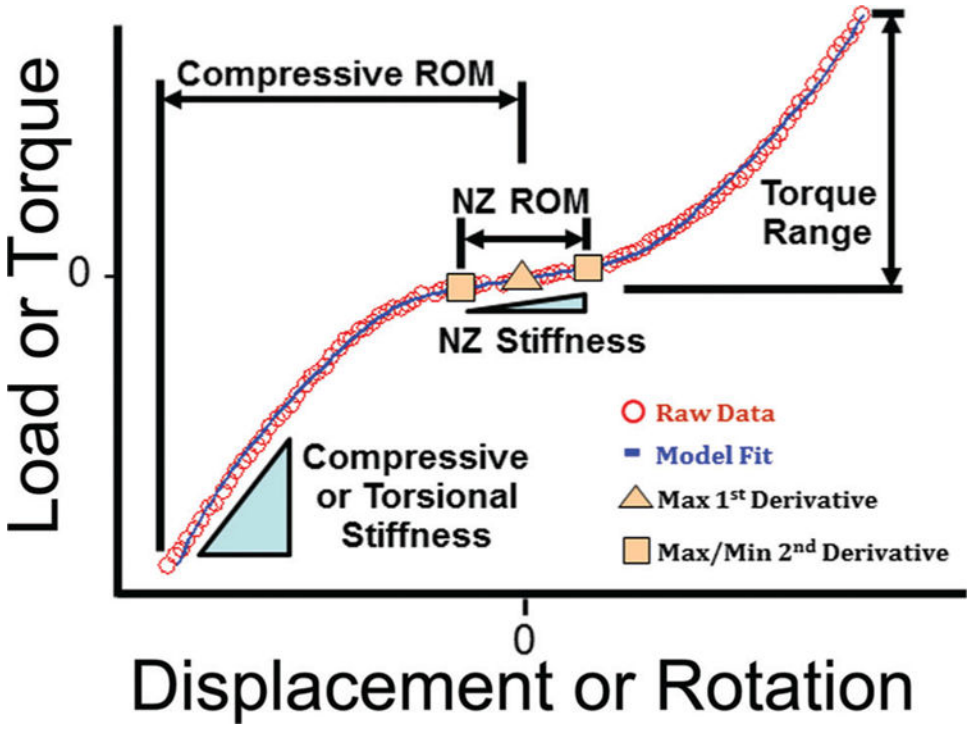

Figure 3.

Loading curves were isolated from the final test cycle to analyze compression and torsion data. Positive (tension or counter-clockwise rotation) and negative (compression or clockwise rotation) curves were made to intersect by shifting each to the load axis to form a composite curve which was subsequently fit to a sigmoid function. The maximum of the 1st derivative (maximum compliance) of the function represents the transition from positive to negative loading. The extremum of the 2nd derivative represent the boundaries of the NZ. NZ stiffness (for compression/tension and torsion) was defined as the slope of the line connecting the point at the each boundary of the NZ. NZ ROM (for compression/tension and torsion) was defined as the displacement between these points. Compressive ROM was defined as the displacement between the inflection point of the curve and the displacement at −1.3 MPa, a value of stress that consistently occurred just prior to the peak stress (the peak stress varied slightly from test to test). Compressive stiffness was defined from the raw data as the slope of the line fit from −1.3 to −0.5 MPa (a value that consistently occurred after the transition region). Torque range was defined as the change in torque from the inflection point of the curve to the maximum torsional load. Torsional stiffness was defined from the raw data by fitting a line from 40% to 90% of the maximum torque for both positive and negative rotations and then averaging the two.

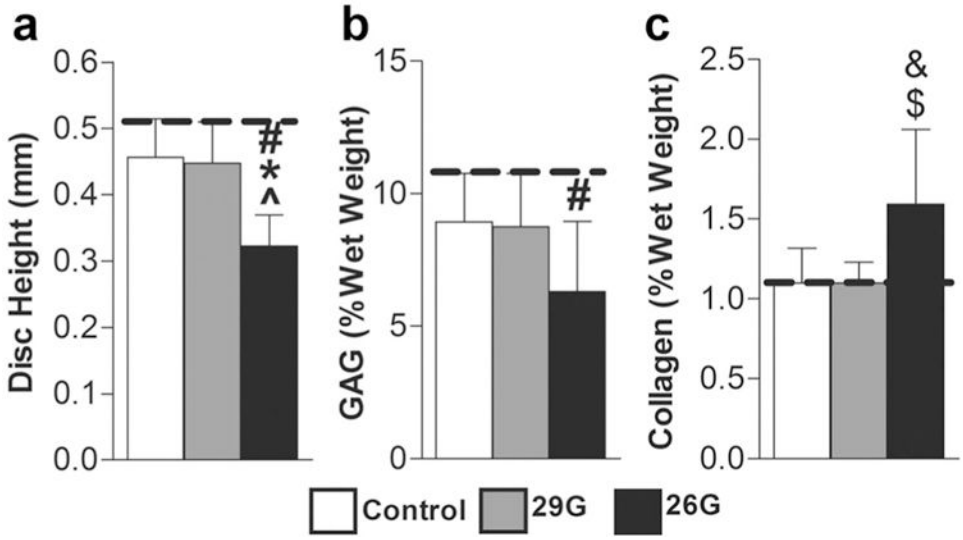

Figure 4.

(a) Disc height (*n* 7/group/timepoint), (b) NP GAG content (*n* 5/group/timepoint), and (c) NP collagen content (*n* 5/group/timepoint) were altered after 8 weeks. Significant differences ($p < 0.05$) are labeled from 0-week control (dotted line) (#), from 8-week control (*), and from 29G (^). Significant trends ($p < 0.10$) are labeled from 8-week control (&) and from 29G ($).

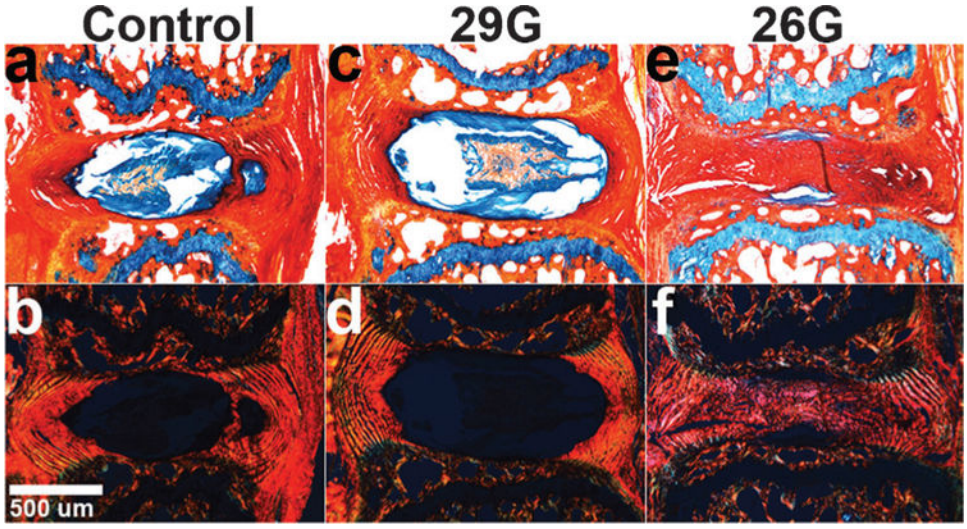

Figure 5.

Alcian Blue/Picrosirius Red stained sagittal sections of 8-week mice viewed under (a–c) brightfield and (d–f) polarized light (n = 2/group/timepoint). (a,d) Control and (b,e) 29G discs were no different at 8 weeks, while (c,f) 26G discs had collapsed height and disorganized lamellae with the presence of collagen-positive stain and lack of GAG-positive stain in the NP.

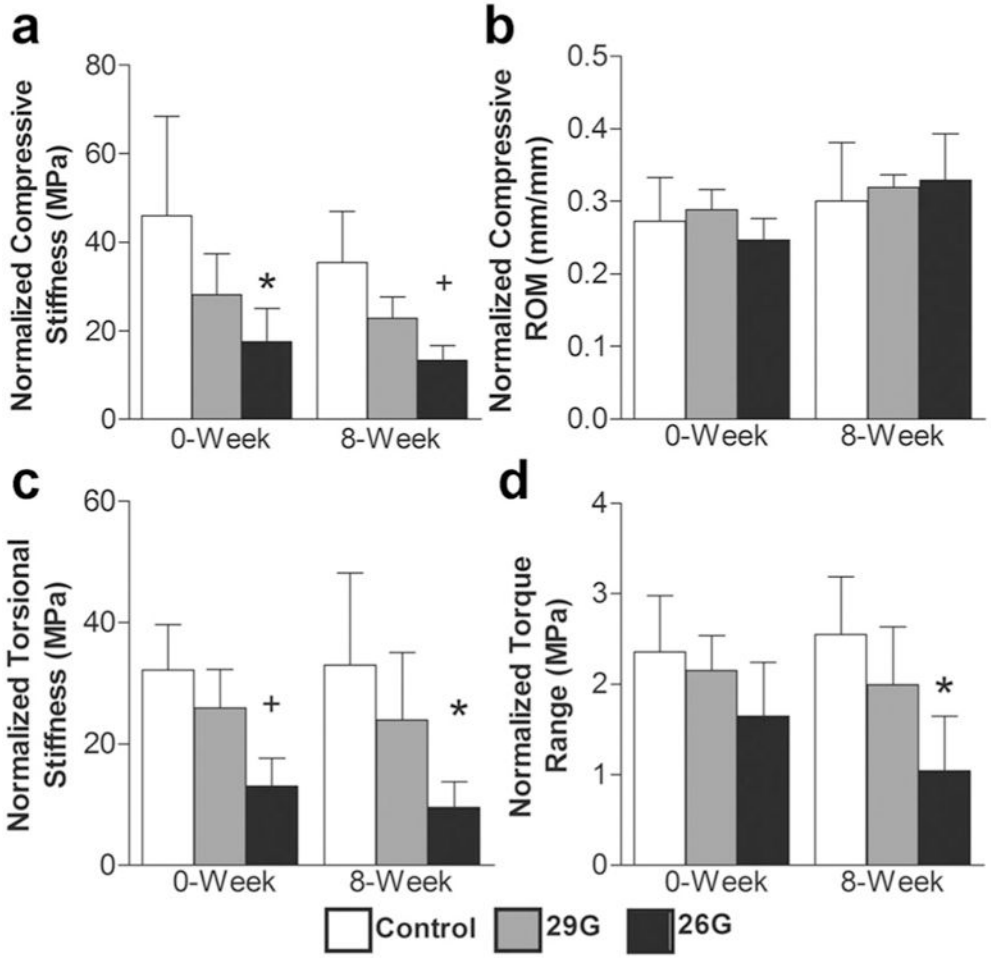

Figure 6.

(a) Normalized compressive stiffness, (b) normalized compressive ROM, (c) normalized torsional stiffness, and (d) normalized torque range ($n = 5$/group/timepoint). Differences from control at each time are labeled as significant ($^{*}p < 0.05$) and trend ($^{+}p < 0.10$).

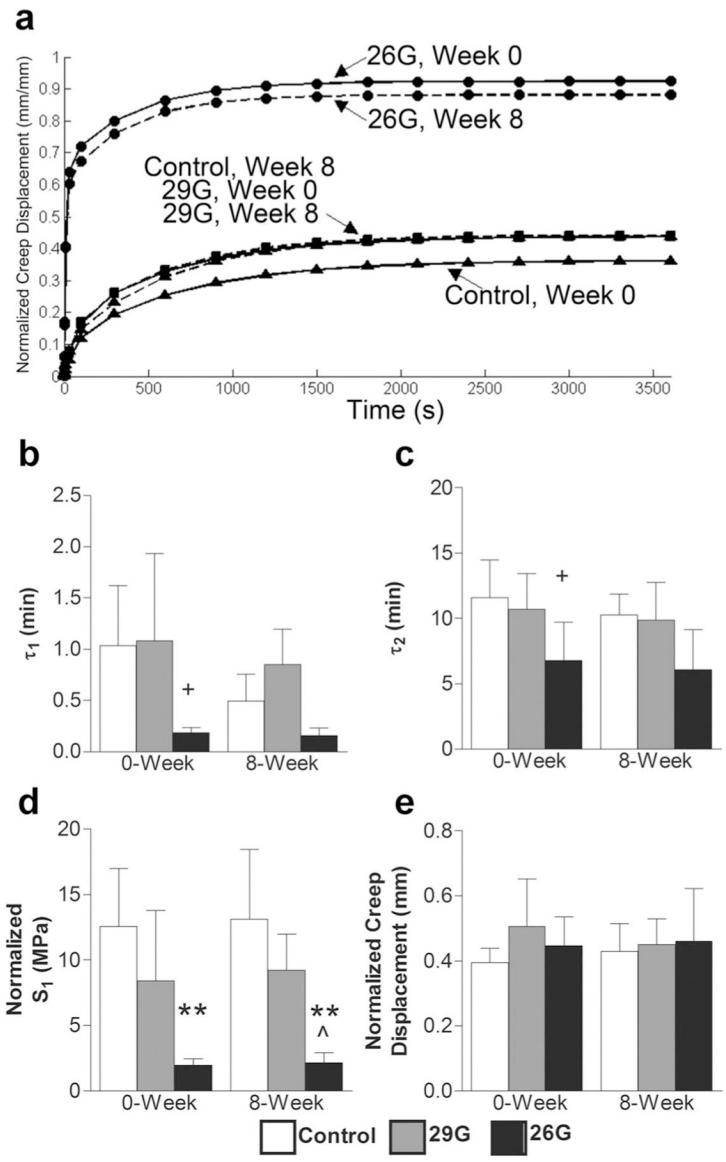

Figure 7.

(a) Average creep curves calculated from mean parameter values in Equation 1. The total response (initial step displacement plus creep displacement) was magnified by puncture while the creep displacement did not change. The data are displayed as: control (triangles), 29G (squares), 26G (circles) with 0-week (solid line) and 8-week (dotted line). (b) Early time constant, τ_1, (c) late time constant, τ_2, (d) normalized early damping stiffness, S_1, (e) and normalized creep displacement ($n = 5$/group/timepoint). Differences from control at each time are labeled as significant ($^{**}p < 0.001$, $^{*}p < 0.05$), and trend ($^{+}p < 0.10$). Significant differences from 29G are labeled as ($^{\wedge}p < 0.05$).